Title

Effect of finite element model loading condition on fracture risk assessment in men and women: The AGES-Reykjavik study

Journal

Bone, 57(1)

ISSN

8756-3282

Authors

Keyak, JH
Sigurdsson, S
Karlsdottir, GS
et al.

Publication Date

2013-11-01

DOI

10.1016/j.bone.2013.07.028

Peer reviewed

Published in final edited form as:
Bone. 2013 November ; 57(1): 18–29. doi:10.1016/j.bone.2013.07.028.

Effect of finite element model loading condition on fracture risk assessment in men and women: The AGES-Reykjavik study

J.H. Keyak[a,b,c,*], **S. Sigurdsson**[d], **G. S. Karlsdottir**[d], **D. Oskarsdottir**[d,e], **A. Sigmarsdottir**[d], **J. Kornak**[f,g], **T. B. Harris**[h], **G. Sigurdsson**[d,e,i], **B. Y. Jonsson**[j], **K. Siggeirsdottir**[d], **G. Eiriksdottir**[d], **V. Gudnason**[d,e], and **T.F. Lang**[f]

[a]Department of Radiological Sciences, University of California, Irvine, CA, USA [b]Department of Biomedical Engineering, University of California, Irvine, CA, USA [c]Department of Mechanical and Aerospace Engineering, University of California, Irvine, CA, USA [d]Icelandic Heart Association Research Institute, Kópavogur, Iceland [e]University of Iceland, Reykjavik, Iceland [f]Department of Radiology and Biomedical Imaging, University of California, San Francisco, CA, USA [g]Department of Epidemiology & Biostatistics, University of California, San Francisco, CA, USA [h]Laboratory of Epidemiology, Demography, and Biometry, Intramural Research Program, National Institute on Aging, Bethesda, MD, USA [i]Landspitalinn University Hospital, Reykjavik, Iceland [j]Department of Orthopaedics, Skane University Hospital, Malmo, Sweden

Abstract

Proximal femoral (hip) strength computed by subject-specific CT scan-based finite element (FE) models has been explored as an improved measure for identifying subjects at risk of hip fracture. However, to our knowledge, no published study has reported the effect of loading condition on the association between incident hip fracture and hip strength. In the present study, we performed a nested age- and sex-matched case-control study in the Age Gene/Environment Susceptibility (AGES) Reykjavik cohort. Baseline (pre-fracture) quantitative CT (QCT) scans of 5500 older male and female subjects were obtained. During 4-7 years follow-up, 51 men and 77 women sustained hip fractures. Ninety-seven men and 152 women were randomly selected as controls from a pool of age- and sex-matched subjects. From the QCT data, FE models employing nonlinear material properties computed FE-strength of the left hip of each subject in loading from a fall onto the posterolateral (F_{PL}), posterior (F_P) and lateral (F_L) aspects of the greater trochanter. For comparison, FE strength in stance loading (F_{Stance}) and total femur areal bone mineral density (aBMD) were also computed. For all loading conditions, the reductions in strength associated with fracture in men were more than twice those in women ($p \leq 0.01$). For fall loading specifically, posterolateral loading in men and posterior loading in women were most strongly associated with incident hip fracture. After adjusting for aBMD, the association between F_P and fracture in women fell short of statistical significance ($p=0.08$), indicating that FE strength provides little advantage over aBMD for identifying female hip fracture subjects. However, in men, after controlling for aBMD, F_{PL} was 424 N (11%) less in subjects with fractures than in controls ($p=0.003$). Thus, in men, FE models of posterolateral loading include information about incident hip fracture beyond that in aBMD.

[*]Corresponding author: Joyce H. Keyak, PhD, Department of Radiological Sciences, University of California, Irvine, CA 92697-5000. Phone: 949-824-9421; Fax: 949-824-8115; jhkeyak@uci.edu. .

Keywords

hip fracture; femur; bone strength; finite element analysis; osteoporosis; quantitative computed tomography

Introduction

Proximal femoral fragility fractures represent the devastating clinical consequence of age-related bone loss. Bone loss results in compartment-specific changes in bone mass, heterogenous changes in bone mineral distribution, and changes in proximal femoral geometry. All of these factors ultimately contribute to loss of bone strength and increased propensity to fracture when the hip is subjected to the loads from a fall.

The risk of hip fracture in an individual depends on the structural integrity of the proximal femur and the likelihood of experiencing forces that exceed this strength. By definition, the strength of a structure is the magnitude of the force required to break the structure. However, the strength (fracture load) of the proximal femur varies depending on the specific force configuration, i.e. the force direction(s) and point(s) of application, which may include forces on the femoral head, greater trochanter, and/or distal aspect of the proximal femur. Thus, the force configuration during normal, physiologic activities such as walking, running, or sitting, is dramatically different than that during a fall onto the greater trochanter. Further, during physiologic activities or impact from a fall, the force magnitudes and directions can be influenced by muscle contraction, subject weight, the height from which a fall occurs (which is often a function of subject height), soft tissue thickness at the impact site, compliance of the impact surface, the degree to which the arm was used to break the fall, and other aspects of fall biomechanics. When evaluating hip fracture risk we may consider the effects of these factors on the magnitudes and directions of the applied forces. However, proximal femoral strength also varies with the directions of the applied forces [1-4], thus complicating the assessment of fracture risk.

Finite element (FE) modeling, which can account for variations in bone strength with force direction, has been studied previously as a method for improved assessment of hip fracture risk [5-6]. However, limited effort has been directed at determining whether the specific force configurations and force directions may provide better fracture risk assessment than others. Previously, using quantitative computed tomographic (QCT) scan-based FE modeling, Orwoll et al. [6] analyzed a lateral fall onto the greater trochanter, but Keyak et al. [5] modeled a posterolateral fall onto the greater trochanter as well as single-limb stance loading on the femoral head to evaluate proximal femoral strength as predictors of hip fracture. Further, the posterolateral fall condition that Keyak et al. studied employed linear FE modeling because a nonlinear method analogous to that for single-limb stance loading had not yet been developed. Thus, due to the different FE methodologies and cohorts of these studies, comparison of the results for multiple loading conditions has not been possible.

To address these inconsistencies in study design, and to evaluate the relationship between bone strength and incident hip fracture across multiple loading conditions, we have carried out the present study. We employed QCT-based FE models with nonlinear material properties to evaluate the proximal femoral strengths in four loading conditions in older male and female hip fracture and control subjects. These strength values included those for loading from a fall onto the posterolateral (F_{PL}), posterior (F_P) and lateral (F_L) aspects of the greater trochanter and, for comparison purposes, the strength for loading in the single-limb stance condition (F_{Stance}) evaluated previously [5]. The objectives were (1) to determine the

extent to which the proximal femoral strength in each loading condition is associated with hip fracture; (2) to determine if these associations differ for men and women; and (3) to determine if each of the proximal femoral strength measures continues to be associated with hip fracture after accounting for areal bone mineral density (aBMD, g/cm^2), which would indicate whether proximal femoral strength includes more information about incident hip fracture than aBMD.

Methods

Subjects

This was a nested age- and sex-matched case-control study from the Age Gene/Environment Susceptibility (AGES) Reykjavik cohort [7]. The AGES-Reykjavik study is an ongoing population-based study of men and women nested in the Reykjavik Study [8-9], and both phases of this study have been described in detail. Baseline QCT scans of 5500 subjects from this cohort who had no metal implants at the level of the hip, but who were otherwise not screened for medical history or medications, were obtained between 2002 and 2006, along with subject age, height, and weight. Although data also included history of medications that might induce changes in bone mineral density (e.g. hormone replacement therapy, bisphosphonates or glucocorticoids), these data were not presented here because they were found not to have a statistically significant effect on the results of our previous [5] and current FE studies. Subjects were followed for 4 to 7 years, through November 15, 2009. Subjects with hip fractures during this period, but without documented hip fracture prior to baseline, were identified through the AGES-Reykjavik Fracture Registry for inclusion in this study [10]. Approximately two controls for each hip fracture subject were randomly selected from a pool of age- and sex-matched subjects in this study. Informed consent was obtained from all participants in the study, which was approved (VSN 00-063) by the National Bioethics Committee in Iceland as well as the Institutional Review Board of the Intramural Research Program of the National Institute on Aging.

Imaging

QCT measurements were performed in the hip using a 4-detector CT system (Sensation 4, Siemens Medical Systems, Erlangen, Germany). A helical study of the hip (120 kVp, 140 mAs, 1-mm slice thickness, pitch = 1, coarsened to 3-mm slice thickness) encompassed the left proximal femur from a point 1 cm superior to the acetabulum to a point 3 to 5 mm inferior to the lesser trochanter (Figure 1a). To enable calibration of the CT Hounsfield units for each voxel to the equivalent calcium hydroxyapatite density (in g/cm^3), all subjects were positioned supine on top of a calibration phantom (Image Analysis, Columbia, KY, USA), which extended from superior to the L1 vertebral body to the mid-femoral shaft (Figures 1a and 1b). The phantom contained calibration cells of 0, 75 and 150 mg/cm^3 of calcium hydroxyapatite. Inclusion of this phantom in the image with the subject is necessary to correct for the effects of variable subject size and composition, and other factors that can influence the CT Hounsfield units.

Finite Element Modeling

From the baseline (pre-fracture) QCT data, we computed the strength of the left hip of each subject in the fracture and control groups using our FE modeling method [11-14], with some modifications to allow nonlinear material modeling for all loading conditions. Four loading conditions were studied, one representing single-limb stance loading [12-14], and three simulating loading from falls onto the posterolateral (PL), posterior (P) and lateral (L) aspects of the greater trochanter [11, 14] (Figures 2a, 2b, and 2c). The models included the entire imaged portion of the proximal femurs.

For single-limb stance loading, heterogeneous linear elastic and nonlinear post-yield material properties computed from QCT-measured bone mineral density (reported previously) were used to describe the stress-strain relationship for each 3-mm cube of bone that was represented by a linear hexahedral finite element measuring 3 mm on a side [13-16]. To maximize precision for fall loading, nonlinear material modeling was used for analysis of fall loading as well. The underlying principles for fall loading were similar to those for our nonlinear FE models of single-limb stance loading [13]. These FE models were designed to compute force values on the femoral head that initially increase, reach a peak value (the proximal femoral strength), and then decrease as displacement is incrementally applied to the femoral head. To achieve this mechanical behavior, the FE models employed heterogeneous isotropic elastic moduli, yield strengths and post-yield properties that were computed from QCT-measured bone mineral density. These material properties were previously measured in the preferred direction of the bone (e.g. in the longitudinal direction for cortical bone). For single-limb stance loading, the elastic modulus, yield strength and plastic modulus values were reduced by 9% to produce FE models that computed accurate proximal femoral strength values [13]. This reduction in properties may account for the effect of material anisotropy, i.e. lower mechanical properties in the non-preferred directions, on the proximal femoral strength. The remaining post-yield parameters did not demonstrate directional dependence, so they were not similarly modified.

Development of the nonlinear FE modeling method for posterolateral fall loading used the same approach as described for single-limb stance loading and was performed on a training set of 8 cadaveric femora that were randomly selected from our previous study of posterolateral fall loading [11]. Initially, the FE models of fall loading used the same isotropic mechanical properties as our models of stance loading so that comparisons between loading conditions could be easily made. However, when posterolateral displacement was incrementally applied to the femoral head to represent posterolateral fall loading, the FE models computed a femoral head force that continually increased, which is inconsistent with fracture of the proximal femur. Noting that the these models employed the von Mises stress failure criterion, the yield stress and post-yield properties were modified until the models exhibited the required mechanical behavior, i.e. computing force values that reached a maximum and then decreased as displacement was applied to the femoral head. The choice of modifications was guided by knowledge that local bone material exhibits reduced strength when stressed in nonphysiologic, sub-optimal directions, which is the case during fall loading. Once the required model behavior was achieved, the final set of yield and post-yield mechanical properties was optimized by iteratively modifying each property until the correlation between the measured and computed proximal femoral strength was maximized. The result of this development procedure was then evaluated on the remaining 9 cadaveric femora (the test set) from the previous study [11].

The ensuing method for calculating the nonlinear mechanical properties of each finite element in FE models of posterolateral fall loading was as follows. The calibrated QCT density (ρ_{CHA}, g/cm^3) of each voxel in the element was used to compute the ash density (ρ_{ash}, g/cm^3) from a linear relationship reported previously ($\rho_{ash} = 0.0633 + 0.887\ \rho_{CHA}$) [13], and ash density was then used to compute mechanical properties that describe a simplified nonlinear stress-strain curve for each voxel (Figure 3, Table 1) [17]. The mechanical properties of the element, which defined the nonlinear stress-strain curve for the element, were then computed by averaging the values of each mechanical property over all voxels in the element, while accounting for partial volume effects by scaling by the volume fraction of each voxel within the element. These FE-computed proximal femoral strength values predicted strength values that were experimentally measured during mechanical testing of cadaveric femora in posterolateral fall loading (training set, r^2=0.92; test set, r^2=0.81 [18]).

These nonlinear mechanical properties were developed for posterolateral fall loading because QCT scan data from cadaveric femora that were mechanically tested in this loading condition already existed for model development and evaluation [11]. For this initial study of multiple loading conditions, these same material properties were employed for posterior and lateral fall loading conditions as well, although ideally, properties specific to each loading condition would be used.

Displacement was applied incrementally to the femoral head, and the reaction force on the femoral head was computed at each increment as the distal end of the model was fully constrained. For the fall models, the surface of the greater trochanter opposite the loaded surface of the femoral head was constrained in the direction of the displacements while allowing motion transversely. The FE-computed bone strength was defined as the maximum force on the femoral head.

Areal Bone Mineral Density

The baseline QCT data for the left hip of each subject in the fracture and control groups, which were calibrated in terms of g/cm^3 equivalent calcium hydroxyapatite density, were also used to compute the aBMD (g/cm^2) in a region of interest comparable to the total femur region of DXA that is used clinically to evaluate osteoporotic hip fracture risk. In a previous study, we reported a strong correlation between the aBMD from QCT and that from DXA aBMD (r=0.935) [5].

Statistical Analysis

The data for men and women were first analyzed separately (R http://www.r-project.org/) using descriptive statistics, and Student's t-tests were used to compare the demographic data, F_{PL}, F_P, F_L, F_{Stance}, and aBMD in the hip fracture and age- and sex-matched control groups. To test for sex differences and to identify the most important determinants of fracture risk, the data for men and women were analyzed together in a single model and multiple regression analysis was performed with each FE-computed bone strength measure serving as the dependent variable. Thus, the coefficient of determination (R^2) indicated the variability in proximal femoral strength that was accounted for by the regression model. We did not evaluate additional strength-related dependent variables, such as an estimated factor of safety (proximal femur strength divided by the applied force) for each loading condition because we found previously (in unpublished work) that parameters normalized by body weight, height or combinations thereof did not affect the findings. Fracture status (yes or no) and demographic parameters, age, height, weight, and sex, were considered as candidate independent variables. Interactions between fracture status and the demographic parameters were also considered. We started with an inclusive model containing the pre-mentioned variables. In refining the model, variables/interactions were tested one at a time and retained only if they were significant at the alpha=0.1 level. If an interaction was retained, the individual variables making up that interaction were also retained, regardless of alpha level, so that the regression would not be forced through zero for those variables. However, results are only reported as significant for $p<0.05$. To determine if each of the proximal femoral strength values were related to fracture status after accounting for aBMD, this procedure was repeated while including as independent variables aBMD and the interactions of aBMD with gender and fracture status. This procedure was then repeated in multiple regression analyses applied separately to men and women. Finally, for comparison purposes, multiple regression analyses with aBMD as the dependent variable were performed separately for men and women, using analogous procedures for the candidate independent variables. In all of these analyses, F_{PL}, F_P, F_L, and F_{Stance}, aBMD, age, height, and weight were standardized by subtracting the mean and dividing by the standard deviation (SD) of the pooled data. No corrections were made for multiple comparisons. However, because only a

single outcome was studied, multiple comparisons only occurred in the context of the search for the optimal predictive set of variables. The final p-values should therefore be interpreted in this context.

Results

Fifty-one men and 77 women suffered hip fractures during the follow-up period. Ninety-seven men and 152 women were selected as control subjects. Of these subjects, 45 male and 72 female hip fracture subjects and 94 male and 145 female control subjects had CT scans suitable for FE analysis. Within each sex, the fracture and control groups were not significantly different with respect to age, height, and weight at the time of the CT scan (Table 2). However, F_{PL}, F_P, F_L, F_{Stance}, and aBMD were significantly lower in each fracture group than in the respective control group (F_L in women, $p=0.012$; all others, $p<0.001$) (Table 2).

Using multiple regression analysis of data for men and women together, while controlling for demographic variables and interactions, revealed that FE strength in all four loading conditions was associated with hip fracture ($0.51<R^2<0.55$; Tables 3-5) and that FE strength was more strongly associated with fracture in men than in women ($p\leq0.01$). In fact, the mean reductions in strength associated with hip fracture in men (stance, 2377 N or 22%; PL fall, 484 N or 13%; P fall, 483 N or 15%; L fall, 574 N or 13%) were more than twice those in women (stance, 975 N or 14%; PL fall, 206 N or 7%; P fall, not significant; L fall, 180 N or 6%). Although the association between F_P and fracture in women was not significant when men and women were examined together, separate analyses for men and women showed that, in women, F_P was the measure most strongly associated with fracture, with a mean strength difference between fracture and control subjects of 184 N (7%). However, when men were analyzed separately, F_P was least associated with fracture, F_{Stance} was most associated with fracture, and F_{PL} was the fall loading condition most associated with fracture, with mean strength differences between fracture and control subjects of 305 N (9%), 2325 N (22%), and 523 N (14%), respectively. Although FE strength in male subjects did not significantly change with age regardless of loading condition or fracture status ($p>0.09$) (Figure 4, Table 4), FE strength for female control subjects in stance, posterolateral fall, posterior fall and lateral fall loading decreased with age ($p\leq0.01$) by 125 N/yr, 26.2 N/yr, 13.9 N/yr and 21.4 N/yr, respectively (1.7%/yr, 0.9%/yr, 0.5 %/yr, 0.7 %/yr, respectively, for an average female control subject) (Figure 4, Table 5). In female fracture subjects, reductions in strength with age were similar to those in control subjects for lateral fall loading ($p>0.10$) but were significantly or nearly significantly smaller in stance ($p=0.032$), posterolateral fall ($p=0.072$) and posterior fall ($p=0.049$) loading (Figure 4, Table 5).

Controlling for aBMD in the regression analyses for men and women together increased the strength of the regression models ($0.53<R^2<0.82$) and revealed an interaction between fracture status and sex for posterior and lateral loading ($p=0.023$ in both cases) (Table 3). Hip strengths in the posterior and lateral conditions were respectively 9% (307 N) and 6% (254 N) less in male fracture subjects than in controls, but there were no such differences for female subjects ($p>0.96$). When F_P and F_L for women were analyzed separately, only the association between F_P and fracture approached statistical significance ($p=0.08$). For posterolateral loading, analyzing men and women together while controlling for aBMD resulted in a nearly significant interaction between fracture status and sex ($p=0.063$). Separate regression analyses for men and women while controlling for aBMD revealed the strongest association between FE strength and fracture in men, with F_{PL} 11% (424 N) less in fracture subjects compared with controls ($p=0.003$), but no such association in women. For single-limb stance loading, the regression analyses for men and women together ($R^2=0.82$)

supported an association between F_{Stance} and fracture ($p<0.001$) and an interaction between fracture and aBMD ($p<0.001$), but no interaction between fracture status and sex (Table 3). We note that this result differs from our previously reported one for the same data (which included an interaction between fracture and sex) [5]; here, we report the regression result with the interaction between fracture and aBMD because this interaction appeared in the regression equations for men and women evaluated separately. In these separate regression equations, there was no association between fracture and F_{Stance} in either men or women ($p=0.14$ and $p=0.064$, respectively), and there was an interaction between fracture status and aBMD ($p=0.013$) in men only, although the interaction in women was only marginally insignificant ($p=.059$) (Tables 4-5). The latter finding indicated that, for each 1 SD increase in aBMD, the difference between F_{Stance} of fracture and control subjects increased by 8% (793 N) in men and by 5% (381 N) in women.

Multiple regression analysis with aBMD as the dependent variable revealed that the mean reductions in aBMD associated with fracture were 0.134 g/cm^2 (15%) in men and 0.071 g/cm^2 (10%) in women (Figure 4, Table 6). In the regression equation for men ($R^2=0.27$), aBMD was constant with respect to age for both fracture and control subjects (≥0.76). For women ($R^2=0.41$), aBMD decreased by 0.0088 g/cm^2/yr ($p<0.001$), or 1.3% per year, in control subjects; however, an interaction between fracture status and age ($p=0.08$) led to a net reduction in aBMD of 0.0039 g/cm^2/yr, or 0.6% per year, in fracture subjects (Figure 4, Table 6).

Discussion

This is the first study to report the relationships between incident hip fracture and FE-computed proximal femoral strength for multiple fall loading conditions representing impact from falls onto various aspects of the greater trochanter. These relationships revealed that, for all loading conditions studied, the *mean* reductions in strength associated with fracture in men were more than twice those in women. Further, in men, the reductions in FE strength due to fracture were independent of age for all loading conditions ($p>0.10$) (Figure 4, Table 4) but, in women, decreased with age in all cases except lateral fall loading (F_{Stance}, $p=0.032$; F_{PL}, $p=0.072$; F_P, $p=0.049$) (Figure 4, Table 5). These differences between FE results in men and women were similar to those for aBMD (Figure 4, Tables 4-6), implying that the sex differences in both FE strength and aBMD largely stem from the original QCT density data (from which the FE strengths and aBMD were computed) and reflect sex differences in proximal femoral density within the DXA total femur region. Despite these differences, the FE-computed hip strength in stance loading was most strongly associated with hip fracture in both men and women. However, stance loading is not directly relevant to hip fracture from a fall onto the greater trochanter and is therefore not of the greatest interest. For fall loading specifically, posterolateral loading in men and posterior loading in women were most strongly associated with incident hip fracture, with regression models accounting for 31% and 26% of the variance in proximal femoral strength, respectively. After adjusting for aBMD, the association between F_P and fracture in women fell short of statistical significance ($p=0.08$), indicating that FE strength provides little advantage over aBMD for distinguishing female hip fracture subjects from female control subjects of the same age. However, in men, proximal femoral strengths in all fall loading conditions remained significant even after accounting for aBMD, with F_{PL} 424 N (11%) less in subjects with fractures than in controls ($p=0.003$). Thus, of the 523 N (14%) reduction in F_{PL} associated with fracture, just 99 N (523 N minus 424 N, or 3% of the bone strength) were uniquely accounted for by aBMD and the remaining 424 N (11% of the bone strength) were due to structural effects that were accounted for by F_{PL}. Finally, although this regression model accounts for 60% of the variance in proximal femoral strength, almost twice that of

the model without aBMD, this result reflects the strong correlation between aBMD and proximal femoral strength rather than an improvement in fracture prediction.

The superior performance, in men, of the FE strengths in fall loading compared with aBMD is not surprising. For many years, aBMD has been used as a surrogate for proximal femoral strength, a key indicator of fracture risk. However, with the emergence of QCT scan-based FE modeling, better estimates of proximal femoral strength have become possible [19]. These models directly and explicitly account for the complex three-dimensional (3-D) geometry and variations in material properties of the proximal femur, thereby allowing them to represent the mechanical response of the bone when forces or displacements are applied. In contrast, aBMD is the mean density in the total femur region, so density variations within that region, and the bone density outside that region, do not affect the value of aBMD. The calculation of aBMD also does not consider forces or displacements, and the 3-D geometry of the proximal femur only indirectly influences aBMD by causing larger bones to have greater aBMD values. Therefore, considering that the FE strengths and aBMD were computed from the same QCT data, the significant FE results after controlling for aBMD must be attributed to differences between the FE and aBMD methodologies. These differences enabled the FE models to provide more robust estimates of proximal femoral strength compared with the total femur aBMD, thereby improving the association with incident hip fracture.

The age-matched design of this study enhanced our ability to explore gender differences in proximal femoral strength and hip fracture as a function of age. In particular, our cross-sectional analysis of age-related FE strength loss by gender and fracture status may explain why proximal femoral strength is strongly associated with incident hip fracture in men but much less so in women. In the youngest male and female subjects, the reductions in strength associated with fracture were comparable (Figure 4). However, more rapid decreases in proximal femoral strength with age in female control subjects compared with those in female fracture subjects (Figure 4, Table 5) caused the reductions in FE strength associated with fracture to vanish in the oldest female subjects for all loading conditions except lateral fall loading. This finding implies that, once the hip bone strengths of all women decrease to a certain level, the most important determinants of hip fracture are those that influence the forces applied to the proximal femur, such as the propensity for falling or fall mechanics. This behavior contrasts dramatically with that of the male subjects whose reductions in bone strength associated with fracture were independent of age. This finding, in combination with the greater proximal femoral strengths in younger men compared with younger women enhanced the age-related differences between men and women. Consistent with previous findings from the AGES-Reykjavik study which showed that the gender disparity in bone loss continued to evolve even in very elderly subjects [20], this finding highlights the need to stratify by age group when evaluating gender differences in fracture prediction.

Although this study was not powered to rigorously compare the regression equations for the four loading conditions, our results suggest that the greatest benefit of using FE analysis instead of aBMD to evaluate hip fracture risk in men may be achieved with posterolateral loading. For this loading condition, after accounting for the effect of aBMD, the percentage reduction in hip bone strength associated with fracture was 11% (424 N), about twice that for posterior loading, 5% (158 N), and lateral loading, 6% (254 N). One might argue that posterolateral loading produced the strongest results in our study because the FE-computed load capacity was optimized in only the posterolateral condition (see Appendix). However, optimization simply maximized the correlation between FE-computed and measured load capacity, which would not induce systematic changes to the FE-computed load capacities in the fracture and/or control subjects. Specifically, for posterolateral loading, optimization caused the FE models to account for about 34% more of the variance in measured load

capacity (corresponding to a standard deviation of 522 N). This improvement in precision increased statistical power, but should not have altered the association between load capacity and fracture status. Similarly, performing additional biomechanical testing and optimizing FE models for posterior and lateral loading would improve precision and increase statistical power for these loading conditions, which would be advantageous in future studies.

Based on biomechanical principles, one might expect that the loading condition with the strongest association between hip bone strength and hip fracture status would most closely represent the conditions of actual hip fracture. However, we must remember that the three "fall" loading conditions modeled here cannot possibly replicate the conditions of an actual fall onto the greater trochanter because our models are relatively simple depictions of the hip fracture process. To clarify this point, consider that fracture is induced in the models by applying displacements to the surface of the femoral head. These displacements are intended to represent the upper body and pelvis, which are initially in motion, pushing against the femoral head. To oppose this motion, our models include constraints on the greater trochanter. These constraints crudely represent the effect of the impact surface which halts motion approximately at the body surface, i.e. at the skin, and then deforms the adjacent soft tissues, causing energy absorption as well as rapid deceleration of the upper body, pelvis and proximal femur. Finally, the effect of the distal femur and lower limb on the proximal femur is represented by fully constraining the distal end of the proximal femur model. However, this part of the leg is in motion during the fall and therefore must decelerate at some point, potentially imposing additional forces on the distal end of the proximal femur during the fracture process. Thus, our models used simple displacements and constraints applied directly to the proximal femoral bone to represent a complex, dynamic process involving the entire body. The models neglected the initial motion and inertial characteristics of the upper body, pelvis and distal limb as well as the distribution, thickness and composition of the soft tissue. Thus, due to the extent of these simplifications, we cannot assume that the loading conditions with the strongest association between hip bone strength and fracture status represent the conditions of actual hip fracture.

Although the biomechanical simplifications of the FE models may obscure the relationship between modeled and actual loading conditions during hip fracture, FE model reproducibility also plays an important role in determining which loading conditions are most strongly associated with hip fracture. Reproducibility of the FE model results depends on many CT scan and FE model input parameters, such as CT scan resolution, reproducibility of the derived geometry and femoral shaft and neck axes, which in turn determine the precision with which the femoral head displacement and greater trochanter constraint directions are specified and applied. Thus, many factors that are unrelated to the biomechanics of hip fracture influence the strength of the regression results. For this reason, we chose to include the posterior fall loading condition even though a posteriorly directed fall would not result in impact on the posterior aspect of the greater trochanter but would instead lead to impact on the ischial tuberosity. Thus, we speculated that, despite the *biomechanically* weak association between actual hip fracture and hip bone strength in posterior fall loading, we might obtain a significant *statistical* association between incident fracture and hip strength in this loading condition because the simple geometric configuration would lead to more precisely determined displacement directions and, consequently, superior reproducibility of the FE-computed load capacity. The significant associations between incident fracture and hip bone strength for both men and women in this loading condition supports this approach (Tables 4 and 5). Similarly, the strong association between incident hip fracture and proximal femur strength in stance loading, which we obtained despite the fact that most hip fractures occur from falls [21], can be at least partly explained by exceptional reproducibility. Our stance loading condition is far superior to that of the fall loading conditions (percent coefficient of variation: stance, 1.6%; PL fall, 4.9%; P

fall, 5.8%; L fall, 5.4% [unpublished data]). which may be the result of applying the femoral head displacements within the coronal plane and/or the absence of constraints on the greater trochanter.

The degree of reproducibility of the FE-computed proximal femoral strength values in both stance and fall loading can be attributed to use of the load capacity, i.e. the maximum force that can be supported by the proximal femur, as the “defination” of the hip bone strength. This study of FE-computed strength and hip fracture incidence is the first to employ the load capacity for a fall loading condition. Other FE studies of fall loading have defined the proximal femoral strength as the force at the onset of fracture of the cortex [22], or the force at which a specific amount of deformation is induced [6]. These alternative approaches were necessary because the FE modeling techniques used in those studies did not model structural collapse, a key characteristic of proximal femoral fracture. Instead, the models predicted that ever-increasing forces and displacements could be applied to the bone, so the load capacity could not be determined. Use of the load capacity instead of the force at the onset of fracture, which we defined as the force at which 15 contiguous elements yielded in our previous study [5], improved the association between FE strength in posterolateral loading and incident hip fracture in men. Most notably, after adjusting for aBMD, FE-computed load capacity in posterolateral loading remained strongly associated with incident hip fracture in men ($p=0.003$), a key improvement over the non-significant association between the force at the onset of fracture and incident hip fracture in our previous study of the same subjects [5].

Using this improved FE modeling method, we can compare our results for lateral fall loading with those of Orwoll et al [6]. Their prospective multicenter study of 3549 male volunteers (mean age, 74 years), included 40 hip fracture and 210 randomly selected, unmatched control subjects. After adjusting for age, body mass index (BMI) and study site, hip bone strength in a lateral fall condition strongly predicted hip fracture even after controlling for aBMD (hazard ratio per SD change for hip fracture=6.5, 95%CI=2.3-18.3). This result is in reasonable agreement with ours, given the different study designs and subject populations. Further, our mean hip bone strength values for lateral fall loading in men were about 73% (control) and 97% (fracture) of those reported by Orwoll et al. This similarity between hip bone strengths in fracture subjects for these two studies, despite differences in FE methodology, subject population, and loading condition (e.g. 15 degrees of anteversion in the previous study which did not exist in our study), is remarkable given the numerous parameters that go into FE modeling of the hip. Further, after adjusting the strength values from the previous study for age using data from Keaveny et al. [23], the mean hip bone strength of our male control subjects was 77% of that reported by Orwoll et al.. However, our mean hip bone strengths for lateral loading in the male and female control groups were 127% and 134%, respectively, of the strength values reported by Keaveny et al. [23] for the mean ages of our control groups. Thus, bone strength values for lateral loading vary considerably and our values fall within the range of those that have been reported previously.

Our study employed 3-D FE models, which is often the case when computing hip bone strength and fracture risk [6, 23]. Three-dimensional models can explicitly represent the 3-D geometry and 3-D distribution of material properties that make each femur structurally and mechanically unique and are therefore considered more robust than two-dimensional (2-D) models. When 2-D models of the proximal femur are used, the bone geometry and material properties are represented as symmetric about the coronal plane, thereby omitting many anatomical features of the bone. The forces applied to a 2-D model also must be directed within the coronal plane which limits the types of studies that can be performed. That said, 3-D FE models do have their drawbacks. Analysis of 3-D models requires greater computing power, data storage and time. More importantly, to construct a 3-D FE model of the

proximal femur, 3-D geometry and material property data are required and are typically obtained from a QCT scan. For in vivo studies, such a scan exposes the subject to ionizing radiation which increases the risk of cancer by an unknown amount. The effective absorbed radiation dose depends on the particular scanner and on the scanner settings, but typically ranges from 1000-3000 microSieverts for the type of volumetric scan typically carried out to generate FE models. Thus, the amount of radiation sustained by a test subject or patient for one of these QCT scans is comparable to the natural background radiation dose received in one year, which varies from 2400-3600 microSieverts, depending on geographic location. In general, it is best to minimize exposure to ionizing radiation, and 2-D FE models make that possible by requiring only 2-D data, e.g. a calibrated radiograph [24] or a DXA scan [25], to construct the model. Thus, 2-D and 3-D modeling each have their strengths and weaknesses, and the best approach for a particular study must be evaluated in the context of the study objectives. The goal of the present study was to investigate the proximal femoral strength in several fall loading conditions, two of which involved forces that were directed outside the coronal plane. The importance of those loading conditions was affirmed because the resulting FE-computed strengths, specifically F_{PL} in men and F_P in women, were the most strongly associated with incident hip fracture in men and women, respectively. Thus, our study objectives precluded the use of 2-D FE models and justified the additional radiation dose to the study participants.

Although our study has a number of important advantages, such as the age- and sex-matched case-control prospective design and analysis of three fall loading conditions, ranging from directly lateral to directly posterior orientations, it has a number of limitations. Some of these limitations were discussed above, such as the lack of optimized density-property relationships for posterior and lateral loading, or were presented previously [5], such as the use of an Icelandic cohort and the underlying simplifications and assumptions of the FE modeling method. Perhaps the most significant limitation is the small number of subjects, especially men, which prevented us from identifying the specific loading conditions that are optimal for assessing fracture risk in men and/or women. However, this limitation did not prevent us from confirming significant associations between proximal femur strength and fracture status for multiple loading conditions and significant differences between men and women. We should also mention as a strength of this study that the direction of the applied displacement vector was defined on a patient-specific basis to be constant with respect to the estimated femoral shaft axis and the coronal plane of each femur. However, this methodology also introduced variability within each category of loading condition to the extent that individual proximal femoral and pelvic anatomy vary, thereby making the distinction between loading conditions less precise. Finally, our analysis of the reductions in strength with age in women with and without fractures was based on the assumption that our cross-sectional data are representative of changes that would occur in individuals over time. Validity of this assumption is supported by the agreement between our current results and those of our previous longitudinal study of age-related changes in proximal femoral strength in men and women which found that decreases in proximal femoral strength with age are much greater in women than in men [26].

In conclusion, FE-computed proximal femoral strength is associated with fracture in all loading conditions that were examined, but the reductions in FE strength associated with fracture in men were more than twice those in women. FE strength in posterolateral loading in men and in posterior loading in women were most strongly associated with incident hip fracture, but only the strength measures in men were associated with hip fracture after accounting for aBMD. Thus, in men, FE models of posterolateral loading include information about incident hip fracture beyond that in aBMD. Further, in women but not in men, in all loading conditions except lateral fall, FE strength decreased with age more rapidly in control subjects than in fracture subjects. As a result, the youngest female control

subjects exhibited greater FE strengths than the youngest fracture subjects, but this difference vanished in the oldest female control and fracture subjects. The significance and complexity of these findings, particularly with respect to gender and age effects, indicate that additional studies of FE modeling for fracture risk assessment in men and women are likely to enhance our understanding of this significant public health problem.

Acknowledgments

This study was supported by NIH/NIA R01AG028832 and NIH/NIAMS R01AR46197. The Age, Gene/Environment Susceptibility Reykjavik Study is funded by NIH contract N01-AG-12100, the NIA Intramural Research Program, Hjartavernd (the Icelandic Heart Association), and the Althingi (the Icelandic Parliament). The study was approved by the Icelandic National Bioethics Committee, (VSN: 00-063) and the Data Protection Authority. The researchers are indebted to the participants for their willingness to participate in the study.

Abbreviations

FE	finite element
$\mathbf{F_{Stance}}$	finite element analysis-computed proximal femoral strength for loading similar to that during single-limb stance
$\mathbf{F_L}$	finite element analysis-computed proximal femoral strength for loading representing a fall onto the lateral aspect of the greater trochanter.
$\mathbf{F_P}$	finite element analysis-computed proximal femoral strength for loading representing a fall onto the posterior aspect of the greater trochanter.
$\mathbf{F_{PL}}$	finite element analysis-computed proximal femoral strength for loading representing a fall onto the posterolateral aspect of the greater trochanter.
L	lateral
P	posterior
PL	posterolateral

References

[1]. Ford CM, Keaveny TM, Hayes WC. The effect of impact direction on the structural capacity of the proximal femur during falls. J Bone Miner Res. 1996; 11:377–383. [PubMed: 8852948]

[2]. Keyak JH, Skinner HB, Fleming JA. Effect of force direction on femoral fracture load for two types of loading conditions. J Orthop Res. 2001; 29:539–544. [PubMed: 11518258]

[3]. Pinilla TP, Boardman KC, Bouxsein ML, Myers ER, Hayes WC. Impact direction from a fall influences the failure load of the proximal femur as much as age-related bone loss. Calcif Tissue Int. 1996; 58:231–235. [PubMed: 8661953]

[4]. Sabick MS, Goel VK. Force needed to fracture and location of fracture region for two simulated fall positions. Trans Orthop Res Soc. 1997; 22:833.

[5]. Keyak JH, Sigurdsson S, Karlsdottir G, Oskarsdottir D, Sigmarsdottir A, Zhao S, Kornak J, Harris TBS,G, Jonsson BY, Siggeirsdottir K, Eiriksdottir G, Gudnason V, Lang TF. Male-female differences in the association between incident hip fracture and proximal femoral strength computed by finite element analysis. Bone. 2011; 48:1239–1245. [PubMed: 21419886]

[6]. Orwoll ES, Marshall LM, Nielson CM, Cummings SR, Lapidus J, Cauley JA, Ensrud K, Lane N, Hoffmann PR, Kopperdahl DL, Keaveny TM. Finite element analysis of the proximal femur and hip fracture risk in older men. J Bone Miner Res. 2009; 24:475–483. [PubMed: 19049327]

[7]. Harris TB, Launer LJ, Eiriksdottir G, Kjartansson O, Jonsson PV, Sigurdsson G, Thorgeirsson G, Aspelund T, Garcia ME, Cotch MF, Hoffman HJ, Gudnason V. Age, Gene/Environment Susceptibility-Reykjavik Study: multidisciplinary applied phenomics. Am J Epidemiol. 2007; 165:1076–1087. [PubMed: 17351290]

[8]. Bjornsson, OJ.; Davidsson, D.; Olafsson, H.; Olafsson, O.; Sigfusson, N.; Thorsteinsson, Th. Report XVIII. Health Survey in the Reykjavik Area - Men. Stages I-III, 1967-1968, 1970-1971 and 1974-1975. Participants, Invitation, Response etc. The Icelandic Heart Association; Reykjavik: 1979.

[9]. Bjornsson, G.; Bjornsson, OJ.; Davidsson, D.; Kristjansson, BT.; Olafsson, O.; Sigfusson, N.; Thorsteinsson, T. Report abc XXIV. Health Survey in the Reykjavik Area - Women. Stages I-III, 1968-1969, 1971-1972 and 1976-1978. Participants, Invitation, Response etc. The Icelandic Heart Association; Reykjavik: 1982.

[10]. Siggeirsdottir K, Aspelund T, Sigurdsson G, Mogensen B, Chang M, Jonsdottir B, Eiriksdottir G, Launer LJ, Harris TB, Jonsson BY, Gudnason V. Inaccuracy in self-report of fractures may underestimate association with health outcomes when compared with medical record based fracture registry. Eur J Epidemiol. 2007; 22:631–639. [PubMed: 17653601]

[11]. Keyak JH, Rossi SA, Jones KA, Skinner HB. Prediction of femoral fracture load using automated finite element modeling. J Biomech. 1998; 31:125–133. [PubMed: 9593205]

[12]. Keyak JH. Improved prediction of proximal femoral fracture load using nonlinear finite element models. Med Eng Phys. 2001; 23:165–173. [PubMed: 11410381]

[13]. Keyak JH, Kaneko TS, Tehranzadeh J, Skinner HB. Predicting proximal femoral strength using structural engineering models. Clinl Orthop Relat Res. 2005; 437:219–228.

[14]. Keyak JH, Koyama AK, LeBlanc A, Lu Y, Lang TF. Reduction in proximal femoral strength due to long-duration spaceflight. Bone. 2009; 44:449–453. [PubMed: 19100348]

[15]. Kaneko TS, Pejcic MR, Tehranzadeh J, Keyak JH. Relationships between material properties and CT scan data of cortical bone with and without metastatic lesions. Med Eng Phys. 2003; 25:445–454. [PubMed: 12787982]

[16]. Kaneko TS, Bell JS, Pejcic MR, Tehranzadeh J, Keyak JH. Mechanical properties, density and quantitative CT scan data of trabecular bone with and without metastases. J Biomech. 2004; 37:523–530. [PubMed: 14996564]

[17]. Keyak JH, Lee IY, Nath DS, Skinner HB. Postfailure compressive behavior of tibial trabecular bone in three anatomic directions. J Biomed Mater Res. 1996; 31:373–378. [PubMed: 8806063]

[18]. Keyak JH, Lang TF. Finite element modeling of proximal femoral load capacity under fall loading. Trans Orthop Resh Soc. 2012; 37:189.

[19]. Cody DD, Gross GJ, Hou FJ, Spencer HJ, Goldstein SA, Fyhrie DP. Femoral strength is better predicted by finite element models than QCT and DXA. J Biomech. 1999; 32:1013–1020. [PubMed: 10476839]

[20]. Sigurdsson G, Aspelund T, Chang M, Jonsdottir B, Sigurdsson S, Eiriksdottir G, Gudmundsson A, Harris TB, Gudnason V, Lang TF. Increasing sex difference in bone strength in old age: The Age, Gene/Environment Susceptibility-Reykjavik study (AGES-REYKJAVIK). Bone. 2006; 39:644–651. [PubMed: 16790372]

[21]. Burge R, Dawson-Hughes B, Solomon DH, Wong JB, King A, Tosteson A. Incidence and economic burden of osteoporosis-related fractures in the United States, 2005-2025. J Bone Miner Res. 2007; 22:465–475. [PubMed: 17144789]

[22]. Bessho M, Ohnishi I, Matsuyama J, Matsumoto T, Imai K, Nakamura K. Prediction of strength and strain of the proximal femur by a CT-based finite element method. J.Biomech. 2007; 40:1745–1753. [PubMed: 17034798]

[23]. Keaveny TM, Kopperdahl DL, Melton LJ 3rd, Hoffmann PF, Amin S, Riggs BL, Khosla S. Age-dependence of femoral strength in white women and men. J Bone Miner Res. 2010; 25:994–1001. [PubMed: 19874201]

[24]. Thevenot J, Pulkkinen P, Koivumaki JEM, Kuhn V, Eckstein F, Jamsa T. Discrimination of Cervical and Trochanteric Hip Fractures Using Radiography-Based Two-Dimensional Finite Element Models. The Open Bone Journal. 2009; 1:16–22.

[25]. Naylor KE, McCloskey EV, Eastell R, Yang L. Use of DXA-Based Finite Element Analysis of the Proximal Femur in a Longitudinal Study of Hip Fracture. J Bone Miner Res. 2013; 28:1014–1021. [PubMed: 23281096]

[26]. Lang TF, Sigurdsson S, Karlsdottir G, Oskarsdottir D, Sigmarsdottir A, Chengshi J, Kornak J, Harris TBS,G, Jonsson BY, Siggeirsdottir K, Eiriksdottir G, Gudnason V, Keyak JH. Age-related

loss of proximal femoral strength in elderly men and women: the Age Gene/Environment Susceptibility Study – Reykjavik. Bone. 2012; 50:743–748. [PubMed: 22178403]

Highlights

- We performed a prospective study of hip fracture in a group of older men and women.
- Finite element-computed hip strength in fracture and control subjects was obtained.
- Stance and posterolateral, posterior and lateral fall loading were analyzed.
- Posterolateral and posterior loading in men and women, respectively, were most strongly associated with hip fracture.

a

b

Fig 1.

The CT scan of a subject positioned supine on top of the calibration phantom. (a) The dashed lines in this scout view indicate the extent of the CT scan, from 1 cm superior to the acetabulum (line labeled “1”) to a point 3 to 5 mm inferior to the lesser trochanter (line labeled “120”), for a total of 120, 1-mm-thick slices for this particular subject. The calibration phantom, rectangular in shape, is also apparent, centered beneath the subject and extending from the lumbar spine to about mid-shaft of the femur. (b) In this CT scan image, the calibration phantom, with its three calibration cells, is visible beneath the subject.

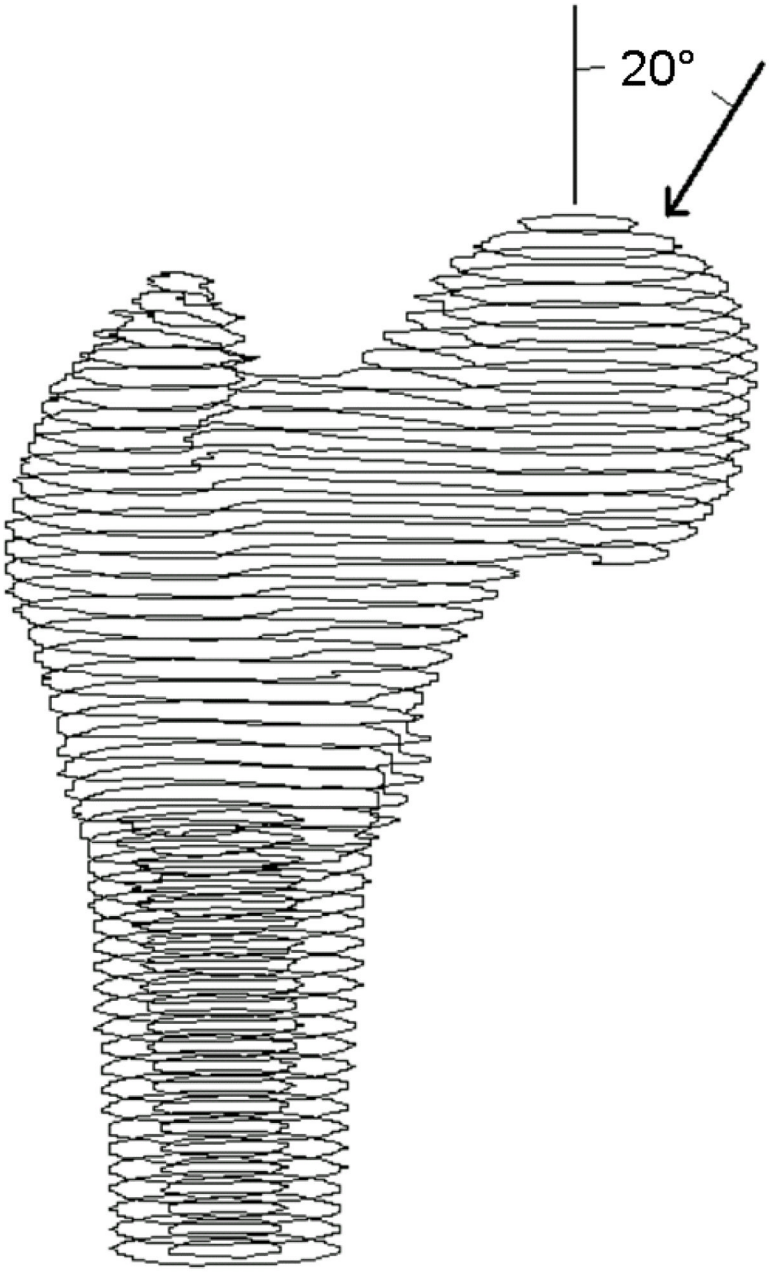

a

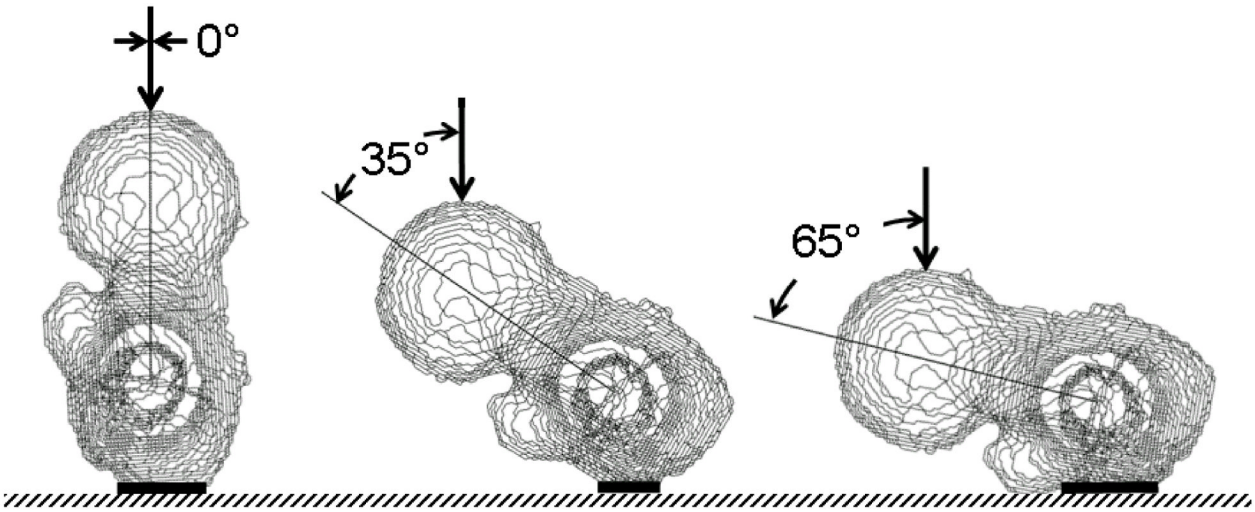

b

Fig 2.

Wireframe plots of contours used to define the proximal femur geometry with the boundary conditions that were applied to the finite element models. (a) For single-limb stance loading displacement was applied to nodes on the femoral head and directed at 20 degrees to the shaft axis in the coronal plane, and the distal end of the proximal femur was fully constrained. (b) For the fall loading conditions, displacement was applied to nodes on the femoral head with motion allowed transversely. Constraints (indicated by the heavy black line) were applied to nodes on the greater trochanter to oppose the applied displacement while allowing for transverse motion. The distal end of the proximal femur was fully constrained. In lateral fall loading (left), the applied displacement was directed within the coronal plane and at 75 degrees to the shaft axis, representing the femoral shaft at 15 degrees to the ground. For posterolateral loading (center), displacement was applied at 35 degrees to the coronal plane and at 80 degrees to the shaft axis. For posterior loading (right), displacement was applied at 65 degrees to the coronal plane and perpendicular to the shaft. Note that these angles are measured within the plane containing the displacement vector and the shaft axis which, for posterolateral loading, does not coincide with any anatomic plane.

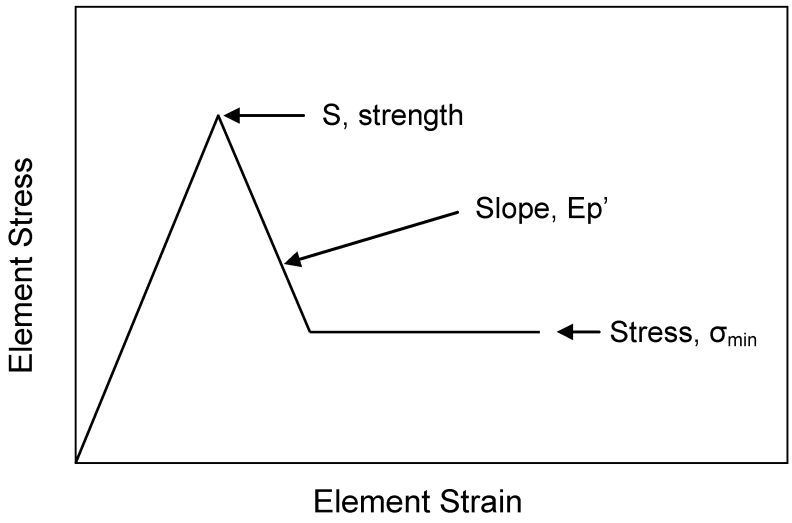

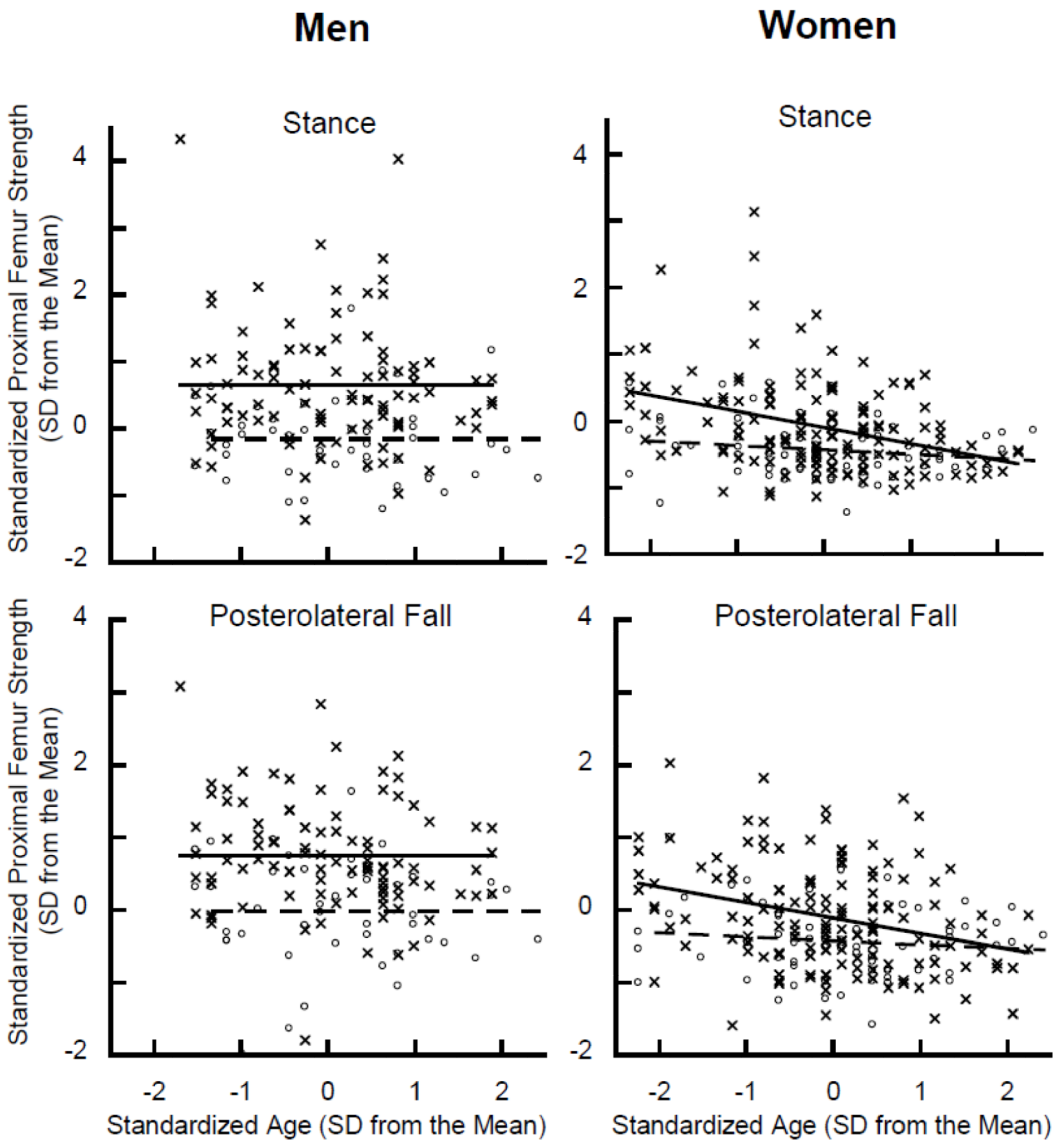

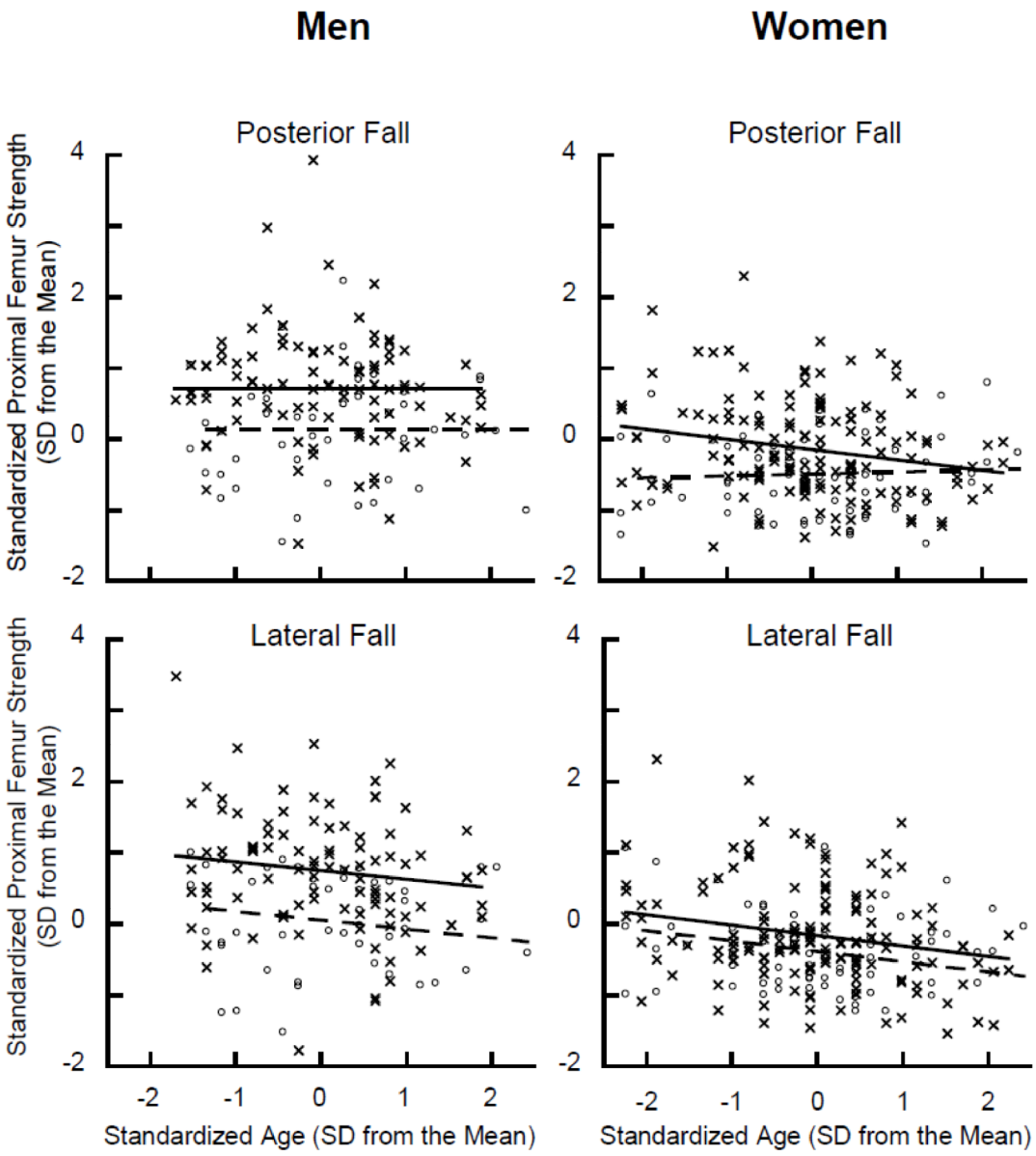

Fig 3.

The stress-strain curve for each finite element includes an elastic region with slope equal to the elastic modulus, E; yield and ultimate strengths, S, which are assumed to coincide; a plastic region with negative slope, E_p' and a perfectly plastic region with a strees of σ_{min}. These parameters are functions of density, as indicated in Table 1.

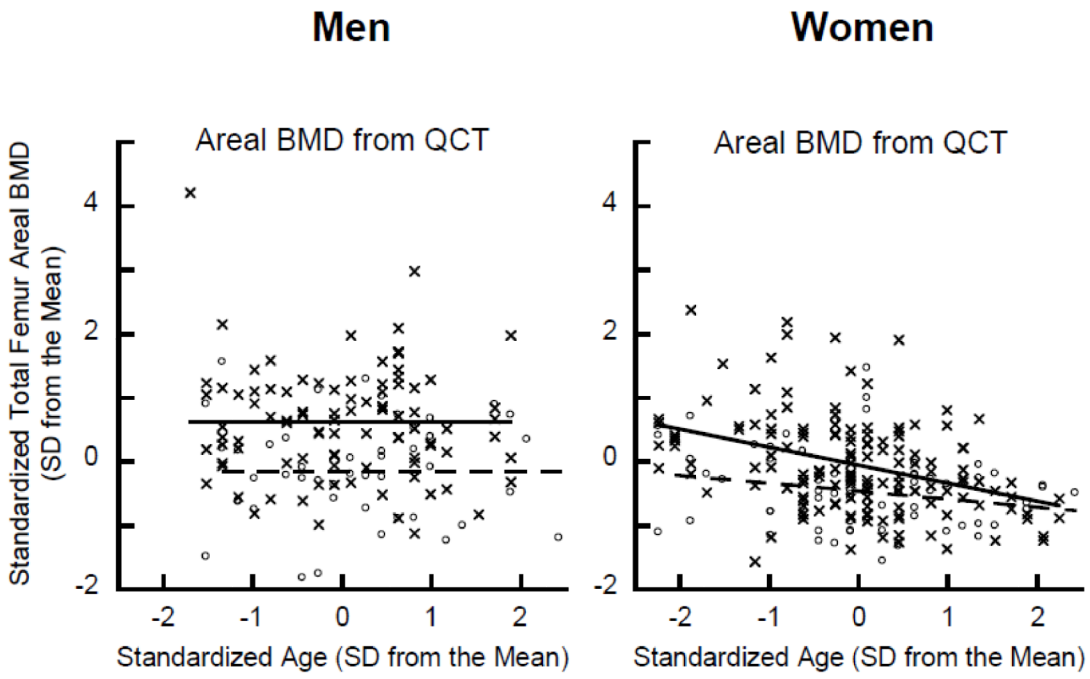

Fig 4.

Proximal femur strength and aBMD versus age in men (left) and women (right) for each loading condition. Data and regression lines for fracture subjects (circles and dashed lines) and control subjects (crosses and solid lines) are standardized by subtracting the mean and dividing by the standard deviation to allow for comparison between loading conditions.

Table 1

Nonlinear material properties used in FE models of fall loading

Parameter	Trabecular Bone Ash density ≤ 0.6037 g/cm^3	Cortical Bone Ash density > 0.6037 g/cm^3
Elastic modulus (MPa)	14,900 (ash density)$^{1.86}$	
Strength (MPa)	102.0 (ash density)$^{1.50}$	23.9
E_p (MPa)[a]	− 125,000 (ash density)$^{1.45}$	− 60,200
E_p' (MPa)	$E_p' = (3 E E_p)/(15 E - 12 E_p)$[b]	
σ_{min} (MPa)	0.42 × Strength	

[a]Prior to specifying the element material properties, E_p was adjusted to account for the smaller size of the finite elements compared with the size of the specimens in which E_p was originally measured [17].

[b]This equation, which was originally developed for trabecular bone [17], was used for both trabecular and cortical bone.

Table 2

Descriptive statistics for subjects with incident hip fracture and the age- and sex-matched controls (approximately two per subject). Statistical significance of differences between cases and controls was established using Student's t-test.

Sex	Measure	Controls						Cases						P
		N[a]	Min	Max	Median	Mean	SD	N[a]	Min	Max	Median	Mean	SD	
Male	age (years)	97	70	90	80.0	79.6	5.2	51	71	93	80.0	80.0	5.6	0.66
	height (cm)	97	162.4	190.5	174.2	174.9	6.6	50	159.2	187.1	173.8	174.6	5.9	0.74
	weight (kg)	97	52.4	135.0	81.6	82.6	14.8	51	50.3	114.0	77.6	79.1	13.9	0.16
	aBMD (g/cm^2)	97	0.511	1.505	0.862	0.867	0.155	51	0.330	1.025	0.735	0.720	0.147	<0.001
	F_{Stance} (N)	94	4772	21,784	9973	10,587	2949	45	3123	12,898	8049	8081	2011	<0.001
	F_{PL} (N)	94	2408	5499	3771	3839	564.0	45	1723	4269	3248	3281	539.2	<0.001
	F_P(N)	94	2149	5078	3321	3314	456.2	44	1766	4155	3013	2977	455.3	<0.001
	F_L(N)	94	2344	6619	4287	4310	736.7	45	1913	4957	3763	3681	618.7	<0.001
Female	age (years)	152	67	92	79.0	79.3	5.7	77	67	93	79.0	79.5	5.9	0.75
	height (cm)	151	139.3	173.0	159.4	159.2	5.6	75	145.1	173.4	160.3	159.6	6.1	0.64
	weight (kg)	151	37.2	112.0	66.3	68.3	13.7	75	39.2	111.2	63.5	64.5	15.1	0.057
	aBMD (g/cm^2)	152	0.338	1.239	0.673	0.696	0.156	76	0.392	0.961	0.592	0.605	0.121	<0.001
	F_{Stance}(N)	145	2978	16,330	6763	7220	2348	72	3085	10,675	5863	6024	1575	<0.001
	F_{PL} (N)	145	1816	4535	2835	2954	555.8	70	1700	4419	2626	2688	435.0	<0.001
	F_P(N)	145	1612	3893	2539	2634	405.7	71	1610	3150	2380	2423	343.6	<0.001
	F_L(N)	145	1771	5386	3197	3244	658.3	72	1945	4896	2985	3016	537.3	0.012

[a]Differences in the number of data points for each measure within each group are due to missing data, CT scans that were inadequate for performing finite element analysis, and/or finite element analyses that did not compute a load capacity.

Table 3

Multiple linear regression results for data from men and women combined, including coefficients of standardized variables, standard errors in parentheses, and p-values in italics. F_{Stance}, F_{PL}, F_P, F_L, aBMD, age, height, and weight were standardized by subtracting the mean and dividing by the standard deviation of the pooled data.[a] Fx=Fracture Status=1 for fracture subjects, 0 for control subjects. Sex = 1 for men, 0 for women. NA=Not applicable (variable was not part of the analysis). "–" indicates that the variable was not included in the model because the p-value would have been greater than 0.10.

Dependent Variable	Regression Coefficients for Standardized Variables (Standard Error) *p value*												R^2
	Fx	**Sex**	**Age**	**Weight**	**Height**	**aBMD**	**Fx:Age**	**Fx:aBMD**	**Fx:Sex**	**Fx:Height**	**Sex:aBMD**	**Intercept**	
						Without Adjustment for aBMD							
F_{Stance}	−0.338 (0.103) *0.001*	0.668 (0.143) *<0.001*	−0.185 (0.050) *<0.001*	0.320 (0.049) *<0.001*	0.138 (0.074) *0.063*	NA	0.135 (0.079) *0.087*	NA	−0.486 (0.165) *0.003*	–	NA	−0.090 (0.073) *0.219*	0.51
F_{PL}	−0.300 (0.100) *0.003*	0.829 (0.137) *<0.001*	−0.150 (0.039) *<0.001*	0.289 (0.047) *<0.001*	0.131 (0.071) *0.067*	NA	–	NA	−0.407 (0.158) *0.010*	–	NA	−0.165 (0.070) *0.019*	0.55
F_P	−0.150 (0.133) *0.261*	0.938 (0.158) *<0.001*	−0.150 (0.051) *0.003*	0.239 (0.048) *<0.001*	0.078 (0.084) *0.355*	NA	0.237 (0.084) *0.005*	NA	−0.756 (0.281) *0.007*	0.311 (0.140) *0.027*	NA	−0.222 (0.078) *0.005*	0.52
F_L	−0.219 (0.102) *0.032*	0.788 (0.141) *<0.001*	−0.184 (0.049) *<0.001*	0.259 (0.048) *<0.001*	0.177 (0.073) *0.016*	NA	0.134 (0.078) *0.084*	NA	−0.480 (0.163) *0.003*	–	NA	−0.171 (0.072) *0.018*	0.52
						With Adjustment for aBMD							
F_{Stance}	−0.183 (0.054) *<0.001*	–	–	0.067 (0.031) *0.036*	0.158 (0.030) *<0.001*	0.801 (0.032) *<0.001*	–	−0.214 (0.056) *<0.001*	–	–	–	0.024 (0.029) *0.402*	0.82
F_{PL}	−0.082 (0.079 *0.302*	0.490 (0.109) *<0.001*	−0.060 (0.031) *0.056*	0.089 (0.039) *0.022*	0.107 (0.055) *0.055*	0.559 (0.038)) *<0.001*	–	–	−0.231 (0.124) *0.063*	–	–	−0.135 (0.055) *0.014*	0.53
F_P	0.006 (0.119) *0.962*	0.655 (0.143) *<0.001*	−0.058 (0.046) *0.209*	0.093 (0.046) *0.043*	0.072 (0.075) *0.336*	0.424 (0.044) *<0.001*	0.172 (0.075) *0.022*	–	−0.570 (0.250) *0.023*	0.281 (0.124) *0.024*	–	−0.189 (0.069) *0.007*	0.62
F_L	0.003 (0.085) *0.969*	0.392 (0.111) *<0.001*	–	0.077 (0.042) *0.063*	0.182 (0.057) *0.001*	0.546 (0.040) *<0.001*	–	–	-0.306 (0.134) *0.023*	–	–	−0.114 (0.057) *0.047*	0.68

[a] Means and standard deviations for each variable (mean±SD): F_{Stance}=7976±2885 N; F_{PL}=3178±685 N; F_P=2815±533; F_L=3535±821; aBMD=0.725±0.174 g/cm^2; age=79.5±5.6 years; height=165.4±9.7 cm; weight=72.7±16.0 kg

Table 4

Multiple linear regression results for men, including coefficients of standardized variables, standard errors in parentheses, and p-values in italics. F_{Stance}, F_{PL}, F_P, F_L, aBMD, age, height, and weight were standardized by subtracting the mean and dividing by the standard deviation of the pooled data.[a] Fx=Fracture Status=1 for fracture subjects, 0 for control subjects. NA=Not applicable (variable was not part of the analysis). "–" indicates that the variable was not included in the model because the p-value would have been greater than 0.10.

Dependent Variable	Regression Coefficients for Standardized Variables (Standard Error) *p value*									R^2
	Fx	**Age**	**Weight**	**Height**	**aBMD**	**Fx:Age**	**Fx:Height**	**Fx:aBMD**	**Intercept**	
					Without Adjustment for aBMD					
F_{Stance}	−0.806 (0.155) *<0.001*	–	0.413 (0.079) *<0.001*	–	NA	–	–	NA	0.652 (0.100) *<0.001*	0.30
F_{PL}	−0.763 (0.136) *<0.001*	–	0.350 (0.070) *<0.001*	–	NA	–	–	NA	0.751 (0.088) *<0.001*	0.31
F_P	−0.572 (0.145) *<0.001*	–	0.364 (0.073) *<0.001*	–	NA	–	–	NA	0.712 (0.093) *<0.001*	0.25
F_L	−0.702 (0.143) *<0.001*	−0.124 (0.073) *0.090*	0.322 (0.076) *<0.001*	–	NA	–	–	NA	0.749 (0.094) *<0.001*	0.29
					With Adjustment for aBMD					
F_{Stance}	−0.161 (0.108) *0.14*	–	0.175 (0.052) *0.001*	–	0.856 (0.063) *<0.001*	–	–	−0.275 (0.110) *0.013*	0.105 (0.076) *0.173*	0.73
F_{PL}	−0.619 (0.207) *0.003*	−0.105 (0.054) *0.055*	0.172 (0.067) *0.011*	−0.075 (0.103) *0.465*	0.530 (0.057) *<0.001*	–	0.310 (0.176) *0.081*	–	0.506 (0.112) *<0.001*	0.60
F_P	−0.297 (0.144) *0.041*	–	0.247 (0.071) *<0.001*	–	0.368 (0.073) *<0.001*	–	–	–	0.486 (0.097) *<0.001*	0.37
F_L	−0.309 (0.127) *0.016*	–	–	0.290 (0.086) *<0.001*	0.558 (0.062) *<0.001*	–	–	–	0.210 (0.111) *0.061*	0.53

[a] Means and standard deviations for each variable (mean±SD): F_{Stance}=7976±2885 N; F_{PL}=3178±685 N; F_P=2815±533; F_L=3535±821; aBMD=0.725±0.174 g/cm^2; age=79.5±5.6 years; height=165.4±9.7 cm; weight=72.7±16.0 kg

Table 5

Multiple linear regression results for women, including coefficients of standardized variables, standard errors in parentheses, and p-values in italics. F_{Stance}, F_{PL}, F_P, F_L, aBMD, age, height, and weight were standardized by subtracting the mean and dividing by the standard deviation of the pooled data.[a] Fx=Fracture Status=1 for fracture subjects, 0 for control subjects. NA=Not applicable (variables was not part of the analysis). "–" indicates that the variable was not included in the model because the p-value would have been greater than 0.10.

Dependent Variable	Regression Coefficients for Standardized Variables (Standard Error) *p value*								R^2
	Fx	**Age**	**Weight**	**Height**	**aBMD**	**Fx:Age**	**Fx:aBMD**	**Intercept**	
				Without Adjustment for aBMD					
F_{Stance}	−0.335 (0.087) *<0.001*	−0.243 (0.052) *<0.001*	0.318 (0.051) *<0.001*	0.136 (0.081) *0.096*	NA	0.177 (0.082) *0.032*	NA	−0.095 (0.069) *0.172*	0.41
F_{PL}	−0.310 (0.094) *0.001*	−0.214 (0.055) *<0.001*	0.257 (0.056) *<0.001*	0.237 (0.088) *0.008*	NA	0.161 (0.089) *0.072*	NA	−0.109 (0.075) *0.147*	0.34
F_P	−0.346 (0.095) *<0.001*	−0.146 (0.056) *0.010*	0.218 (0.055) *<0.001*	0.204 (0.088) *0.022*	NA	0.175 (0.089) *0.049*	NA	−0.147 (0.075) *0.052*	0.26
F_L	−0.218 (0.095) *0.023*	−0.146 (0.048) *0.002*	0.267 (0.056) *<0.001*	0.178 (0.089) *0.046*	NA	–	NA	−0.166 (0.076) *0.030*	0.29
				With Adjustment for aBMD					
F_{Stance}	−0.124 (0.067) *0.064*	–	–	0.119 (0.043) *0.006*	0.770 (0.345) *<0.001*	–	−0.132 (0.069) *0.059*	−0.048 (0.040) *0.226*	0.79
F_{PL}	–	–	–	0.192 (0.061) *0.002*	0.636 (0.042) *<0.001*	–	–	−0.111 (0.050) *0.026*	0.60
F_P	−0.144 (0.083) *0.084*	–	–	0.149 (0.066) *0.025*	0.515 (0.048) *<0.001*	–	–	−0.145 (0.060) *0.017*	0.47
F_L	–	–	–	0.177 (0.063) *0.005*	0.589 (0.044) *<0.001*	–	–	−0.129 (0.052) *0.014*	0.53

[a] Means and standard deviations for each variable (mean±SD): F_{Stance}=7976±2885 N; F_{PL}=3178±685 N; F_P=2815±533; F_L=3535±821; aBMD=0.725±0.174 g/cm^2; age=79.5±5.6 years; height=165.4±9.7 cm; weight=72.7±16.0 kg

Table 6

Multiple linear regression results when aBMD was the dependent variable, including coefficients of standardized variables, standard errors in parentheses, and p-values in italics. aBMD, age, height, and weight were standardized by subtracting the mean and dividing by the standard deviation of the pooled data.[a] Fx=Fracture Status=1 for fracture subjects, 0 for control subjects. "–" indicates that the variable was not included in the model because the p-value would have been greater than 0.10.

Dependent Variable	Group	Regression Coefficients for Standardized Variables (Standard Error) *p value*						R^2
		Fx	Age	Weight	Height	Fx:Age	Intercept	
aBMD	Men	−0.772 (0.145) *<0.001*	–	0.321 (0.076) *<0.001*	–	–	0.615 (0.097) *<0.001*	0.27
aBMD	Women	−0.409 (0.095) *<0.001*	−0.283 (0.056) *<0.001*	0.414 (0.052) *<0.001*	–	0.158 (0.091) *0.084*	−0.054 (0.057) *0.341*	0.41

[a] Means and standard deviations for each variable (mean±SD): aBMD=0.725±0.174 g/cm^2;age=79.5±5.6 years; height=165.4±9.7 cm; weight=72.7±16.0 kg